Observational Study

Medicine®

OPEN

Biological characteristics of ^{18}F-FDG PET/CT imaging of cerebral alveolar echinococcosis

Amina Yibulayin, MD, Xiao-Hong Li, MD, Yong-De Qin, MD*, Xiao-Yan Jia, MD, Qi-Zhou Zhang, MD, Yu-Bin Li, MD

Abstract

This study aims to analyze the characteristics of ^{18}F-fluorodeoxyglucose positron emission tomography/computed tomography (^{18}F-FDG PET/CT) for cerebral alveolar echinococcosis (CAE).

Twenty-five CAE patients underwent ^{18}F-FDG PET/CT, and the diagnosis was confirmed by clinical and surgical pathology. The ^{18}F-FDG PET/CT results were subject to visual and semiquantitative analysis, and the difference in ^{18}F-FDG SUV_{max} for lesions among the 3 types of CAE was evaluated.

In the 25 CAE patients, 62 lesions were detected by ^{18}F-FDG PET/CT, and these lesions were classified into 3 types, according to the characteristics of the lesion's uptake of ^{18}F-FDG on PET images: type I, 17 lesions, FDG was concentrated into a mass radioactive distribution in the CAE foci; type II, 28 lesions, FDG presented a annular concentrated radioactive distribution around the CAE foci; type III, 17 lesions, FDG in the CAE foci presented a radioactive distribution with defects and sparse areas. The difference in ^{18}F-FDG SUV_{max} between type I and type II CAE was not statistically significant ($P > .05$), the difference in ^{18}F-FDG SUV_{max} between type I and type III CAE was statistically significant ($P < .001$), and the difference in ^{18}F-FDG SUV_{max} between type II and type III CAE was statistically significant ($P < .001$);

The ^{18}F-FDG PET manifestations of CAE are classified into 3 types. Both type I and type II may have invasive activity, while the lesions of type III CAE show that the focus is relatively stable or at a stationary phase. If there are no definite alveolar echinococcus focus in other sites, these patients can temporarily delay the treatment. It is recommended that the patient should undergo whole body PET/CT once a year to dynamically observe the bioactivity and size of type III CAE lesions and assess the presence of new echinococcus lesions in the rest of the body.

Abbreviations: 18F-FDG PET/CT = ^{18}F-fluorodeoxyglucose positron emission tomography/computed tomography, CAE = cerebral alveolar echinococcosis, *E granulosus* = *Echinococcus granulosus*, *E multilocularis* = *Echinococcus multilocularis*, ELISA = enzyme-linked immunosorbent assay, OSEM = ordered-subsets expectation maximization, SNK-q = Student–Newman–Keuls-q, SUV_{max} = maximum standardized uptake value.

Keywords: ^{18}F-fluorodeoxyglucose positron emission tomography/computed tomography, cerebral alveolar echinococcosis, deoxyglucose, radioactive nuclide

1. Introduction

Echinococcosis is a serious zoonotic disease caused by Echinococcus parasiting in the body of intermediate hosts, such as humans and some animals. Echinococci that cause human echinococcosis mainly include 2 kinds: *Echinococcus granulosus* (*E granulosus*) and *Echinococcus multilocularis* (*E multilocularis*). Alveolar echinococcosis is an infectious disease caused by *E multilocular* infection, which seriously threatens human health. The disease is distributed globally, and mainly distributed in the northern hemisphere. In cattle-producing area of Northern Europe, North Africa, Middle East, and Northwest China, the incidence is relatively high. At present, with the rapid increase in population migration and the number of immigrants worldwide, the disease is distributed all over the world. When people eat the diet with Echinococcus eggs, or eat food with eggs which is stick on tableware and fingers, the eggs are hatched into oncospheres in the duodenum, which are then activated by bile and pancreatic juice, and enter the portal system. The liver is the most common target organ to be affected. Although its histopathology manifests as a benign disease caused by parasitic infection, it often shows characteristics similar to the invasive growth of malignant tumors, and is extremely likely to invade the adjacent organs and develop distant metastasis,[1,2] which can often affect the lung, abdominal cavity, pelvic cavity, spleen, kidney, brain, and other tissues and organs. Patients with cerebral echinococcosis accounted for 0.5% to 3% of patients with echinococcosis,[3–5] and patients with alveolar echinococcosis accounted for about 1% of patients with cerebral echinococcosis. Almost all of these involvements are secondary to the blood metastasis of hepatic alveolar echinococcosis, and are rare in clinic and the prognosis is poor. In the present study, 25 patients with cerebral alveolar echinococcosis (CAE), who were treated in our hospital from July

Editor: Michael Masoomi.

AY and X-HL are co-first authors.

The authors have no conflicts of interest to disclose.

Department of Nuclear Medicine, The First Affiliated Hospital of Xinjiang Medical University, Urumqi, China.

* Correspondence: Yong-De Qin, Department of Nuclear Medicine, The First Affiliated Hospital of Xinjiang Medical University, No. 1 Liyushan Road, Urumqi 830054, China (e-mail: qyd199013@163.com).

Medicine (2018) 97:39(e11801)

Received: 4 May 2018 / Accepted: 16 July 2018

http://dx.doi.org/10.1097/MD.0000000000011801

2012 to October 2017, were enrolled. The diagnosis was confirmed by clinical and surgical pathology. The PET/CT image features and pathological results were subject to contrast, in order to analyze the ^{18}F-FDG biological characteristics of CAE.

2. Data and methods

2.1. Subjects

In the present study, 25 patients with CAE, who were treated in our hospital from July 2012 to October 2017, were enrolled. Among these patients, 11 patients were Han nationality, 6 patients were Tibetan nationality, 5 patients were Kazak nationality, 2 patients were Mongolian nationality, and 1 patient was Hui nationality. Furthermore, among these 25 patients, 16 patients were male and 9 patients were female, and the average age of these patients was 41.5 ± 10.4 years old. The diagnosis of 10 patients was confirmed by surgical pathology, while the diagnosis of the remaining 15 patients was comprehensively based on clinical history, serum hydatid enzyme-linked immunosorbent assay (ELISA), head magnetic resonance imaging (MRI) and follow-ups, and complete clinical data.

2.2. Methods

This study was conducted in accordance with the Declaration of Helsinki. This study was conducted with approval from the Ethics Committee of The First Affiliated Hospital of Xinjiang Medical University. Written informed consent was obtained from all participants.

2.2.1. Imaging methods. All 25 CAE patients underwent cranial ^{18}F-fluorodeoxyglucose positron emission tomography/computed tomography (^{18}F-FDG PET/CT). ^{18}F-FDG was produced by the GE MINItrace QILING cyclotron and the positron drug production line, and was synthesized by an automatic synthesis module. The radiochemical purity was >95%. The imaging equipment used was the Discovery VCT PET/CT imaging device, which was purchased from GE by the First Affiliated Hospital of Xinjiang Medical University. Each patient underwent brain ^{18}F-FDG PET/CT imaging after providing a signed informed consent. Fasting for more than 6 hours was required before imaging, and fasting blood glucose at the end of the finger was controlled within 7 mmol/L. Under the resting state, 7.4 MBq/kg (body weight) of ^{18}F-FDG was intravenously injected. At 1 hour after injection, under the eye-closing resting state, CT scan was performed from the cranial top to the lower end of the cerebellum. CT image acquisition parameters: voltage, 120 kV; tube current, 330 mA; detector collimating aperture, 64×0.625 mm; thickness of scanning slice, 2.5 mm; slice gap, 2.5 mm; speed, 0.6 ms/rotation; pitch, 0.983; scanning duration, 5 to 10 seconds. PET 3D acquisition was performed in the same scanning range of CT. The acquisition time for each bed was 5 minutes. After the acquisition was completed, the PET images were subject to attenuation correction using CT data. The transect, coronal, and sagittal images and PET/CT fusion images were reconstructed using the ordered-subsets expectation maximization (OSEM) algorithm.

2.2.2. Image analysis. The images were separately analyzed by 2 physicians of nuclear medicine with PET/CT diagnostic experience. First, the image quality was evaluated using the visual method. After understanding the normal physiological uptake, normal variation and artifact, the presence of abnormal FDG concentration in and around the lesion was observed. Then, the biological boundaries of the foci of CAE were outlined, the number and sizes of the lesions were recorded, and the characteristics of the ^{18}F-FDG distribution in the lesions were analyzed. Next, the maximum standardized uptake value (SUV_{max}) in the lesion was measured, and the exact location of the focus was determined based on the anatomical information provided by CT images from the same machine.

2.3. Statistical analysis

Statistical analysis was conducted using statistical software SPSS 17.0. Measurement data were statistically presented as mean ± standard deviation. The ^{18}F-FDG SUV_{max} of the 3 types of CAE were compared using one-way analysis of variance. If there was a general difference, pairwise comparison was conducted using the Student–Newman–Keuls-q (SNK-q) test.

3. Results

3.1. General outcomes and treatment situations

Among the 25 patients, 23 patients had a history of primary hepatic alveolar echinococcosis, while 2 patients had primary cerebral alveolar echinococcosis. A total of 62 lesions were detected by ^{18}F-FDG PET/CT, and the diameters ranged within 10 to 50 mm. A total of 11 patients (44%) had single lesions: lesions were located in the cerebral hemisphere in 9 patients, a lesion was located in the cerebellum in 1 patient, and a lesion was located in the thalamus in one patient. A total of 14 patients (56%) had multiple lesions: 44 lesions were located in the cerebral hemisphere, 4 lesions were located in the cerebellum, 2 lesions were located in the basal ganglia, and 1 lesion was located in the thalamus. Among the 25 patients, 22 patients had lung transfer, 4 patients had kidney transfer, 4 patients had atrial and ventricular transfer, 1 patient had pleural transfer, 1 patient had splenic transfer, and 2 patients had mediastinal transfer. Serum hydatid ELISA revealed that 23 patients were positive (among these patients, 10 patients were strongly positive) and 2 patients were negative.

Among the 25 patients, 10 patients underwent surgical treatment. Among these 10 patients, 4 patients received resection of single CAE lesion, and 6 patients had multiple lesions, in which only part of these lesions were resected. Furthermore, in these 10 patients, a total of 17 cerebral transferring lesions were resected and pathologically proven to be alveolar echinococcosis. Nine of these lesions presented with obvious necrosis and multinucleated giant cell response, and were surrounded by inflammatory granulation tissue. In 3 patients, after the resection of hepatic alveolar echinococcosis, the rest of the body had no definite alveolar hydatid focus. PET/CT results suggested that the transferring foci of echinococcosis in the brain had no clear metabolic activity. Furthermore, these patients presented without clinical manifestations of elevated intracranial pressure. Therefore, these patients did not receive any treatment. It is recommended that the patient should undergo whole body PET/CT once a year to dynamically observe the bioactivity and size of type III cerebral alveolar echinococcosis lesions and assess the presence of new echinococcosis lesions in the rest of the body. The remaining 12 patients were treated with drug therapy, such as oral use of albendazole, combined with dehydration, hormone and antiepileptic therapy. After the symptoms were relieved, these patients were discharged from the hospital.

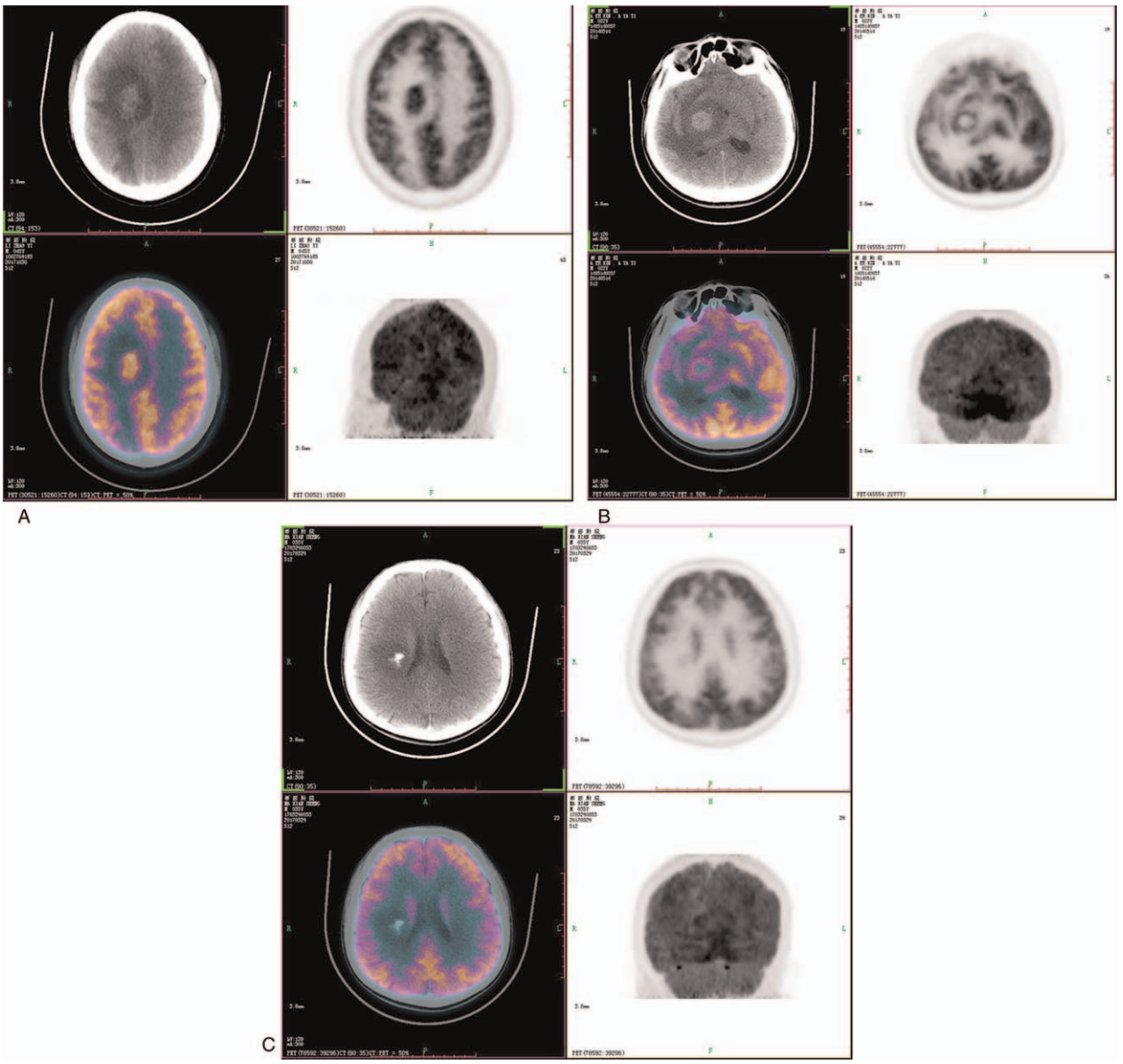

Figure 1. The classification diagram of cerebral alveolar echinococcosis (CAE). (A) I-mode CAE. It presents a 45-year-old male patient. The ^{18}F-FDG PET/CT revealed that in lesions in the right parietal lobe, FDG presented a homogeneous solid mass concentration in a radioactive distribution, and this was pathologically proven to be CAE. (B) II-mode CAE. It presents a 22-year-old male patient. The ^{18}F-FDG PET/CT revealed that in lesions in the right basal ganglia, FDG presented an annular radioactive concentration. These were pathologically proven to be CAE lesions with obvious necrosis and multinuclear giant cell response, which were surrounded by inflammatory granulation tissue. (C) III-mode CAE. It presents a 32-year-old male patient. The ^{18}F-FDG PET/CT revealed that in lesions in the right basal ganglia, FDG presented a radioactive concentration with sparse areas and defects. ^{18}F-FDG PET/CT = ^{18}F-fluorodeoxyglucose positron emission tomography/computed tomography, CAE = cerebral alveolar echinococcosis.

3.2. PET/CT characteristics of the CAE lesion

The lesions of CAE were classified into 3 types, according to the characteristics of the lesion's uptake of ^{18}F-FDG on the PET images: type I, 17 lesions, FDG was concentrated into a mass-shaped radioactive distribution in the CAE foci (Fig. 1A); type II, 28 lesions, FDG presented a annular concentrated radioactive distribution around the CAE foci (Fig. 1B); type III, 17 lesions, FDG in the CAE foci presented a radioactive distribution with defects and sparse areas (Fig. 1C). On nonenhanced CT images, the foci manifested as space occupying soft tissue density. There were spotted or irregular calcifications in some of the lesions, and there were obvious edema (54 cases) and a space occupying effect (Figs. 1 and 2) in the surrounding area.

3.3. Statistical results

The quantitative analysis results of ^{18}F-FDG SUV_{max} were compared among the 3 types of CAE lesions. The ^{18}F-FDG SUV_{max} of type I CAE lesion was 9.62 ± 3.17, while the ^{18}F-FDG SUV_{max} of type II CAE lesion was 9.94 ± 4.05, and the difference between these 2 was not statistically significant ($P > .05$). Furthermore, the ^{18}F-FDG SUV_{max} of type I CAE lesion was significantly higher than that of type III CAE lesion (2.33 ± 0.54), and the difference between these 2 was statistically significant ($P < .001$). The ^{18}F-FDG SUV_{max} of type II CAE lesion was significantly higher than that of type III CAE lesion, and the difference between these 2 was statistically significant ($P < .001$) (Table 1).

Table 1

Variation analysis of ^{18}F-FDG SUV_{max} in the patients with 3 types of CAE lesion ($\bar{x} \pm s$).

The type of the lesion	The number of the lesion	SUV_{max}*	F	P
Type I	17	$9.62 \pm 3.17^{\dagger}$	33.690	<.001
Type II	28	$9.94 \pm 4.05^{\dagger}$		
Type III	17	2.33 ± 0.54		

^{18}F-FDG PET/CT = ^{18}F-fluorodeoxyglucose positron emission tomography/computed tomography, CAE = cerebral alveolar echinococcosis, SUV_{max} = maximum standardized uptake value.

* Standardized uptake value.

Compared with the type III.

† $P < .001$.

4. Discussion

4.1. Application of ^{18}F-FDG PET/CT and other imaging techniques in CAE

MRI is superior to CT in the diagnosis of CAE due to its unique high resolution for soft tissue. However, the biological activity of the boundary and invasive growth of lesions cannot be accurately judged by MRI. A preliminary study revealed that novel imaging techniques, such as contrast-enhanced ultrasound, dual energy/energy spectrum CT, and MRI diffusion weighted imaging, are expected to be able to detect the blood supply of the lesion and determine its metabolic activity. However, these imaging methods cannot be popularized at present. Multicenter, large-sample observations should be further carried out in patients in different stages to determine the reliability of the clinical application of these novel technologies.[6]

^{18}F-FDG PET/CT is presently well recognized as a noninvasive detection tool for evaluating the metabolic activity of alveolar echinococcus lesions via 3-dimensional imaging.[7,8] Delayed imaging (3 hours after injection of ^{18}F-FDG) can reduce false negatives and improve the sensitivity in determining the metabolic activity of echinococcus lesions.[9] PET/CT imaging can clearly detect the location, morphology and number of alveolar echinococcus lesions, as well as the invasion to peripheral organs. The FDG uptake of CAE indicates the biological activity of the lesion, which can help accurately outline the boundary of the lesion. According to the intake of FDG and the clinical symptoms of the patient, the next step treatment regimen can be determined.

4.2. Characteristics of PET/CT of CAE

In the present study, the difference in ^{18}F-FDG SUV_{max} between type I and type II CAE was not statistically significant. Among the 17 excised lesions (SUV_{max} was 7.6–15.4), 9 lesions had obvious necrosis, multinucleated giant cell response, and peripheral inflammatory granulation tissue formation. Furthermore, PET/CT revealed an annular high intake of FDG. In the remaining 8 lesions, 2 lesions presented with mass-shaped high uptake of FDG, while 6 lesions presented an annular high intake of FDG. These results reveal that the degree of uptake of FDG in transferring alveolar echinococcosis was not related to its distribution, which could be characterized by a crumby or annular radioactive distribution, and all may have invasive activity. In the present study, a patient with a left occipital cerebral transferring echinococcosis was followed-up. The manifestation of CT was hybrid density space occupying combined with calcification, and the manifestation of PET was annular uneven high uptake of FDG at the periphery of the lesion. The lesion gradually increased within 16 months, the long diameter grew from 2.5 to 3.1 cm, the FDG uptake of the lesion continued to have an annular uneven high uptake, and the SUV_{max} slightly increased from 8.3 to 10.2 (Fig. 2).

In the present experiment, the manifestations of the CT of 17 type I lesions with mass-like uptake of FDG was more uniform in soft tissue occupying, and the CT value was within 52–78. In the other 17 type III lesions with sparse areas or defects of FDG uptake, the center was mostly calcified at different degrees, and the CT value was within 61–373. The investigators considered that these foci were presently relatively stable or at a stationary phase. If there was no definite alveolar echinococcus focus in other parts, these patients could temporarily not receive any treatment. It is recommended that the patient should undergo whole body PET/CT once a year to dynamically observe the bioactivity and size of type III cerebral alveolar echinococcosis lesions and assess the presence of new echinococcosis lesions in the rest of the body. If the size, number, and bioactivity of lesions of the type III alveolar echinococcosis do not change, and there was no new echinococcosis lesions in the rest of the body, it is recommended to continue the follow-up; if the volume of the original type III CAE lesion enlarges, or there is a new echinococcosis lesion in the brain or whole body PET/CT suspects that there are new echinococcosis lesions in other tissues and organs, it should be immediately treated once it is diagnosed. However, the characteristics of brain alveolar echinococcosis lesion in which CT reveals calcification cannot be considered as an obsolete lesion or lesion at a stationary phase, it is still necessary to determine the treatment regimen in combination with the intake of FDG.

In the present study, among the 25 patients, the ELISA results for serum echinococcosis revealed that 23 patients were positive. Among the 2 negative patients, 1 patient had multiple transferring CAE lesions, which was characterized by the absence of ^{18}F-FDG uptake, while the other patient had a single transferring cerebral echinococcosis lesion, which presented an annular uneven high uptake of ^{18}F-FDG (SUV_{max} was 8.3), and resected primary hepatic alveolar echinococcosis lesions, there was no definite transferring lesions in other parts of the body. Therefore, it could not be excluded in the negative result of ELISA for serum echinococcosis that the focus had no biological activity.[3]

4.3. Exploration of ^{18}F-FDG uptake mechanism of transferring CAE

Studies have revealed that in the ^{18}F-FDG PET/CT imaging of alveolar echinococcosis, FDG was perfused to micrangia through blood circulation, and participated in cellular metabolism. The manifestation was an annular or crumby radioactive concentration zone in the periphery of the lesion. The denser the blood vessels were, the more concentrated the radioactive distribution became.[9,10] The cytokines secreted by the alveolar hydatid can promote microvascular growth in peripheral granulation tissue.[11,12] Therefore, the SUV_{max} of tissues surrounding the focus is also affected by the surrounding granulomas with different sizes.[13,14] An experiment verified that FDG is mainly uptaken by immune cells in the foci of alveolar echinococcosis.[15] The more obvious the infiltration of inflammatory cells, such as macrophages and mononuclear cells, the more the FDG uptake also became.[16] In the study conducted by Li et al,[17] some of the alveolar echinococcosis lesions had a high SUV_{max}. However, the

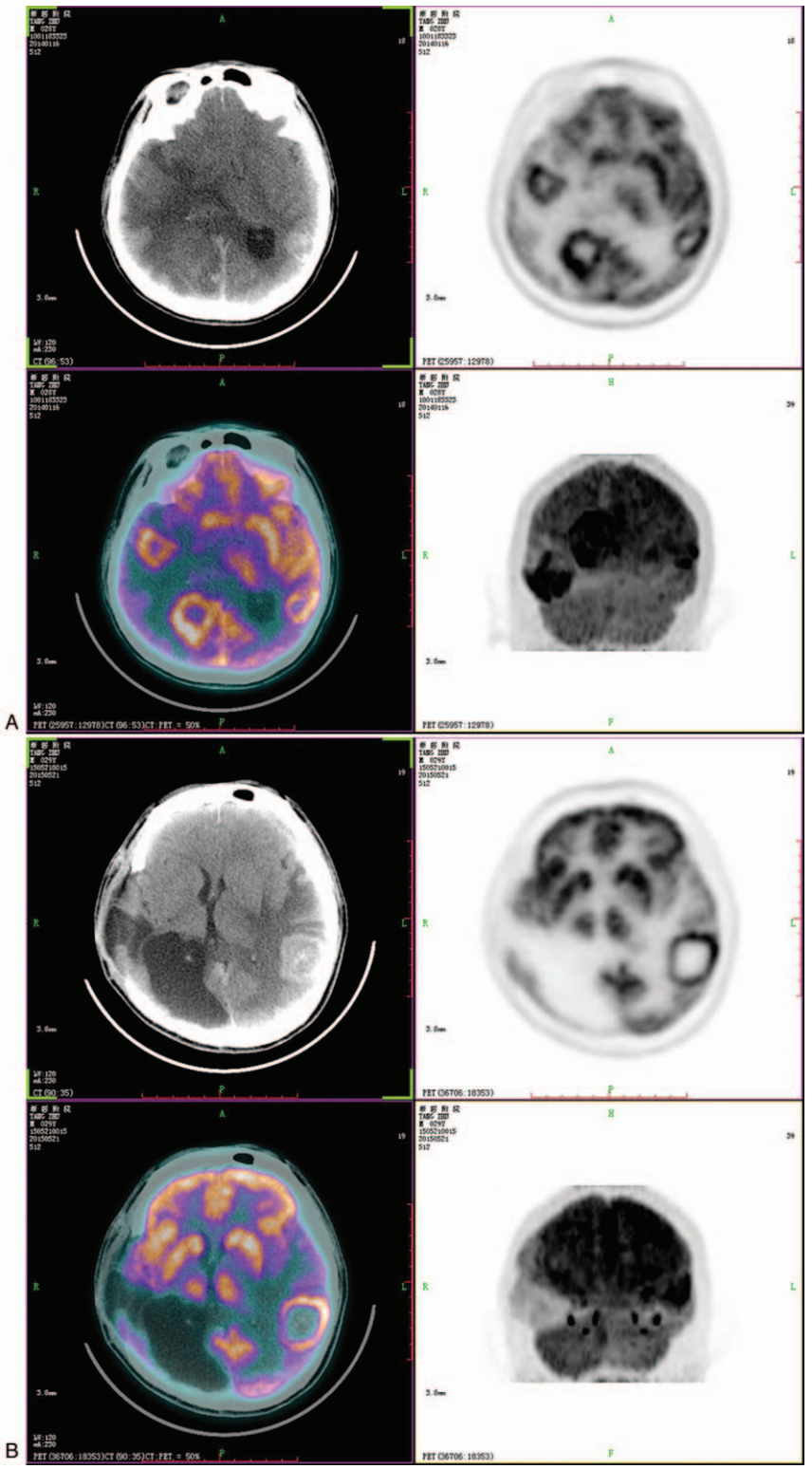

Figure 2. The follow-up diagram of patients with CAE. (A) Brain ^{18}F-FDG PET/CT image in January 2014. It presents a 26-year-old male patient. The ^{18}F-FDG PET/CT conducted in January 2014 revealed that in the right temporal lobe and bilateral occipital lobes, FDG was concentrated in an annular radioactive distribution around the lesion. The size of the lesion in the left occipital lobe was approximately 2.5 × 2.1 cm, and the SUV_{max} was 8.3. The transferring lesions of CAE in the right temporal lobe and right occipital lobe were resected in the right month. Pathological findings revealed CAE with obvious necrosis and collagen proliferation, and a large amount of inflammatory cell infiltration. (B) Brain ^{18}F-FDG PET/CT image in May 2015. It presents a 27-year-old male patient. The ^{18}F-FDG PET/CT conducted in May 2015 revealed changes in the transferring lesions of CAE in the right temporal lobe and right occipital lobe after resection. The size of the transferring CAE lesion in the left occipital lobe was approximately 3.1 × 2.6 cm, and was surrounded by a annular radioactive concentration of FDG. The SUV_{max} was 10.2. The lesion in the left occipital lobe was resected in February 2016. Pathological findings revealed CAE with obvious necrosis, calcification and collagen proliferation, and a large amount of inflammatory cell infiltration. ^{18}F-FDG PET/CT = ^{18}F-fluorodeoxyglucose positron emission tomography/computed tomography, CAE = cerebral alveolar echinococcosis, SUV_{max} = maximum standardized uptake value.

count of microvascular density in CD34 staining was not high. This also indirectly revealed that the SUV indicated by PET/CT is the common result of the density of new blood vessels, nodular granuloma formation, macrophages, neutrophils, lymphocytes, eosinophils, plasma cells, and other inflammatory cell infiltrations.[18] In the present experiment, the results revealed that the crumby uptake of transferring CAE did not appear in the periphery of the lesion, but in the lesion instead. This may be related to its histologic manifestation. When the coagulated necrotic zone in the central of the lesion is rare, the lesion itself can be characterized by a solid crumby uptake. Otherwise, the lesion would present an annular high intake of FDG.

Reuter used PET to follow-up the changes in ^{18}F-FDG metabolism in the foci of hepatic alveolar echinococcosis,[19] and the results revealed that the focus was relatively stable when the edge of the liquefaction area of the focus maintained sparse and reduced radionuclide, since the radionuclide in the edge of the liquefaction area of the focus changed from sparse and reduced to local concentrated, and the infiltration of the lesion increased. The result revealed that the "added value infiltration zone" on the edge of the lesion or the active focus area is an important sign to reflect the development trend of the lesion. Prospective evaluation is presently ongoing to delineate the usefulness and best modalities of PET/CT follow-ups in monitoring disease activity, in order to optimize therapeutic management and re-assess the long-term treatment with benzimidazoles as a final goal, on the basis of clearly discriminating imaging findings.[20,21] The dynamic observation of biological active areas with different energy metabolism in CAE lesions can not only be used as a guide in determining the treatment regimen, but also provide new clinical significance in recognizing the infiltration mechanism of CAE to the surrounding tissues.

Author contributions

Conceptualization: Amina Yibulayin, Yong-De Qin.
Data curation: Amina Yibulayin, Xiao-Hong Li, Xiao-Yan Jia, Qi-Zhou Zhang, Yu-Bin Li.
Formal analysis: Amina Yibulayin, Xiao-Hong Li, Xiao-Yan Jia, Qi-Zhou Zhang, Yu-Bin Li.
Investigation: Amina Yibulayin, Xiao-Hong Li, Xiao-Yan Jia, Qi-Zhou Zhang, Yu-Bin Li.
Methodology: Amina Yibulayin, Yong-De Qin.
Project administration: Yong-De Qin.
Resources: Xiao-Hong Li, Xiao-Yan Jia, Qi-Zhou Zhang, Yu-Bin Li.
Software: Xiao-Hong Li, Xiao-Yan Jia, Qi-Zhou Zhang, Yu-Bin Li.
Supervision: Yong-De Qin.
Writing – original draft: Amina Yibulayin.
Writing – review & editing: Xiao-Hong Li, Yong-De Qin, Xiao-Yan Jia, Qi-Zhou Zhang, Yu-Bin Li.

References

[1] Craig P. Echinococcus multilocularis. Curr Opin Infect Dis 2003;16: 437–44.
[2] Piarroux M, Piarroux R, Giorgi R, et al. Clinical features and evolution of alveolar echinococcosis in France from1982 to 2007: results of a survey in 387 patients. J Hepatol 2011;55:1025–33.
[3] Shakeri , Vahedi , Payman . Cerebral echinococcosis in the children and young adults. Neurosurg Quart 2007;17:241–4.
[4] Bükte Y, Kemaloglu S, Nazaroglu H, et al. Cerebral hydatid disease: CT and MR imaging findings. Swiss Med Wkly 2004;134:459–67.
[5] Lunardi P, Missori P, Ercoli L. Multiple cerebral hydatid disease: case report with magnetic resonance imaging study. Neurosurgery 1993;32: 152.
[6] Liu WY, Delabrousse É, Blagosklonov O, et al. Innovation in hepatic alveolar echinococcosis imaging: best use of old tools, and necessary evaluation of new ones. Parasite 2014;21:74.
[7] Crouzet J, Mantion GA, Thevenot T, et al. Personalized management of patients with inoperable alveolar echinococcosis undergoing treatment with albendazole: usefulness of positron-emission-tomography combined with serological and computed tomography follow-up. Clin Microbiol Infect 2010;16:788–9.
[8] Reuter S, Schirrmeister H, Kratzer W, et al. Pericystic metabolic activity in alveolar echinococcosis: assessment and follow-up by positron emission tomography. Clin Infect Dis 1999;29:1157–63.
[9] Caoduro C, Porot C, Vuitton DA, et al. The role of delayed 18F-FDG PET imaging in the follow-up of patients with alveolar echinococcosis. J Nucl Med 2013;54:358–63.
[10] Parsak CK, Demiryurek HH, Inal M, et al. Alveolar hydatid disease: imaging findings and surgical approach. Acta Chir Belg 2007;107:572–7.
[11] Elsebaie SB, ElSebae MM, Esmat ME, et al. Modified endocystectomy versus pericystectomy in *Echinococcus granulosus* liver cysta: a randomized controlled study and the role of specific anti-hydatid IgG4 in detection of early recurrence. J Egypt Soc Parasitol 2006;36:993–1006.
[12] Bauder B, Auer H, Schilcher F, et al. Experimental investigation on the B and T cell immune response in primary Alveolar echinococcosis. Parasite Immunol 1999;21:409–21.
[13] Zhang L, Zhang SJ, Cao YW, et al. The correlation between osteopontin and metastasis of hepatic *Echinococcus multilocularis* infection. Zhongguo Ji Sheng Chong Xue Yu Ji Sheng Chong Bing Za Zhi 2011;29:33–6.
[14] Silva MA, Mirza DF, Bramhall SR, et al. Treatment of hydatid disease of the liver. Dig Surg 2004;21:227–34.
[15] Porot C, Knapp J, Wang J, et al. Development of a specific tracer for metabolic imaging of alveolar echinococcosis: a preclinical study. Conf Proc IEEE Eng Med Biol Soc 2014;2014:5587–90.
[16] Bostanci B, Tetik C, Terzi C, et al. Efficiency of ultrasound in the detection of the viability of hydatid cysts in the liver. Surg Laparosc Endosc Percutan Tech 1999;9:392.
[17] Li XH, Zhang QZ, Xie B, et al. A Study on the tissue infiltration mechanism of 18F-FDG PET/CT in determining biological boundaries of hepatic alveolar echinococcosis. Clin Exp Med 2016;9:8204–10.
[18] Love C, Tomas MB, Tronco GG, et al. 18F-FDG PET of infection and inflammation. Radiographics 2005;25:1357–68.
[19] Reuter S, Grüner B, Buck AK, et al. Long-term follow-up of metabolic activity in human alveolar echinococcosis using FDG-PET. Nuklearmedizin 2008;47:147–52.
[20] Bresson-Hadni S, Grenouillet F, Knapp J, Demonmerot F, Richou C, Vuitton DA, Millon L, the FrancEchino and EchinoVista networks. 2014. Reference-centre network for the care management of alveolar echinococcosis: the FrancEchino and EchinoVista experience, in Proceedings of the International Symposium "Innovation for the Management of Echinococcosis," Besan, March 27–29, 2014, Vuitton DA, Millon L, Gottstein B, Giraudoux P, Editors. Parasite, 21, 28, 63–4.
[21] Vuitton DA, Bresson-Hadni S. Alveolar echinococcosis: evaluation of the therapeutic strategies. Exp Opin Orphan Drugs 2014;2:67–86.